Remote Sensing Letters, 2015
Vol. 6, No. 8, 597–603, http://dx.doi.org/10.1080/2150704X.2015.1062158

Taylor & Francis
Taylor & Francis Group

Remote sensing of spatial-temporal distribution of suspended sediment and analysis of related environmental factors in Hangzhou Bay, China

Lina Cai[a,b,c], DanLing Tang[a,c]*, Xiaofeng Li[d], Hong Zheng[b], and Weizeng Shao[b]

[a]*Research Center for Remote Sensing of Marine Ecology & Environment, State Key Laboratory of Tropical Oceanography, South China Sea Institute of Oceanology, Chinese Academy of Sciences, Guangzhou, China;* [b]*Laboratory of Marine Acoustics and Remote Sensing, Zhejiang Ocean University, Zhoushan, Zhejiang, China;* [c]*School of Ocean Sciences, University of Chinese Academy of Sciences, Beijing, China;* [d]*GST, NOAA/NESDIS/STAR, College Park, MD, USA*

(*Received 4 March 2015; accepted 3 June 2015*)

In this study, a total of 37 images of Landsat Operational Land Imager/Thematic Mapper/Enhanced Thematic Mapper plus were adopted to delineate the qualitative changes of Suspended Sediment Concentration (SSC) in Hangzhou Bay, China. Combined with in-situ SSC, remote sensing reflectance of the water (R_{rs}), water depth and simulated currents, the influence of both seabed topography and tidal currents on the SSC distribution was analysed. The results showed: (1) four High SSC Areas (HSA) and two Low SSC areas (LSA) in Hangzhou Bay. (2) SSC has a negative correlation with bathymetry, which is especially obvious during mid to late period of flood tide. HSAs appear in the shallow water (3–7 m depth) area, while the LSAs distribute in the deep water area (10–15 m depth). (3) The surface SSC distribution during the mid to late period of flood tide can help us estimate the topography information. The results of this paper can be used to other coastal embayments similar to Hangzhou Bay.

1. Introduction

Suspended sediment has important impacts on water quality and marine ecology of coastal waters (Ilyina et al. 2006; Mayer et al. 1998), and also affects the seabed morphology and shipping channels (Webster and Lemckert 2002).

Hangzhou Bay (Figure 1), whose water is optically dominated by suspended sediments (Wang et al. 2012), is located in the coastal waters of East China Sea. Many factors have contribution to the Suspended Sediment Concentration (SSC) distribution in Hangzhou Bay, where suspended sediments come partly from Yangtze River (Shenliang, Guoan, and Shilun 2003) due to the sediments transported by freshwater injection and the East China Sea coastal flow (Jilan and Kangshan 1989). Qiantang River also transports suspended sediment to Hangzhou Bay. Furthermore, besides the offshore coastal currents and tidal flow carrying suspended sediment to the bay area, sediments re-suspension also contributes to the turbidity in the study area (Chen and Wang 2008; Tang et al. 1998). Till now, the relationship between SSC spatial distribution and the seabed bathymetry of Hangzhou Bay is not well understood due to lack of data.

In this study, we investigate the SSC distribution in Hangzhou Bay, analysing both in-situ remote sensing reflectance of the water (R_{rs}) and high- resolution Landsat data of Operational Land Imager (OLI)/Enhanced Thematic Mapper plus (ETM+)/Thematic

*Corresponding author. Email: lingzistdl@126.com

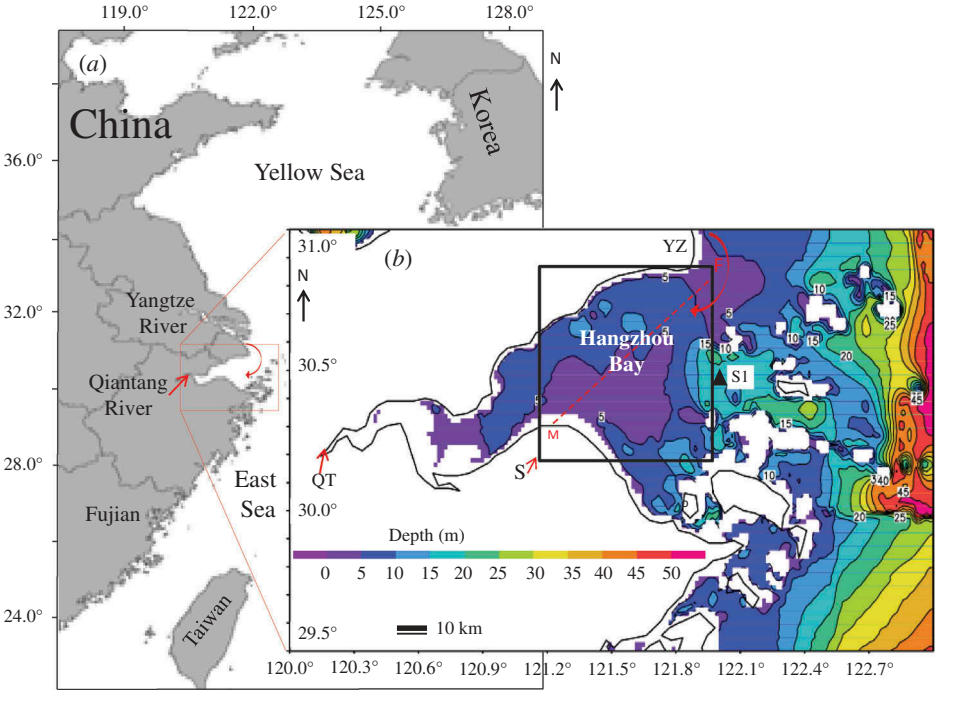

Figure 1. (*a*) Map of the Hangzhou Bay. MF in (*b*): The transect of qualitative SSC. The shading indicates the bathymetry. QT: Qiangtang River entrance; YZ: Yangtze River entrance. Black square (S) in Figure 1(*b*): The position of sampling area on 30 March 2014.

Mapper (TM). We also investigate the contribution of seabed topography and tidal currents to SSC distribution, using the bathymetry data, in-situ SSC, and simulated tidal currents.

2. Data processing

2.1. *In-situ data*

The R_{rs}, SSC and water depths of study area were measured during surveys conducted in Hangzhou Bay from 6:00 a.m. to 6:00 p.m. on 30 March 2014. Sampling area was shown in Figure 1(*b*). The water depths were measured using Acoustic Doppler Current Profilers (ADCP). The in-situ measurements are used as follows: Firstly, in situ R_{rs} and corresponding SSC were used to find out the sensitive wave bands to SSC; Secondly, in-situ water depth and synchronously measured SSC were used to analyse their relationship.

The R_{rs} was obtained using an ISI921VF visible, near infrared (NIR), high spectral radiometer with a spectral range of 380–1080 nm.

The SSC, defined as the dry mass of particles per unit volume of water (units are mgl^{-1}), was determined following the steps of Qiu (2013).

The in-situ R_{rs} and SSC showed that NIR bands indicate the highest correlation between SSC and R_{rs}, with the correlation coefficient r around 0.8175. NIR band is more sensitive to SSC than other bands whose correlation coefficients are 0.6015 (blue), 0.598 (green), 0.712 (red), respectively, in SSC dominated water in Hangzhou Bay (SSC more than 150 mgl^{-1}).

2.2. Remote sensing data

Thirty-seven Landsat OLI/ETM+/TM images obtained during 1990–2014 were adopted to analyse SSC spatial distribution in Hangzhou Bay.

Based on in-situ SSC and water R_{rs}, the qualitative SSC of satellite images was retrieved using OLI band 5 and TM/ETM band 4 following Jiang's method (Jiang, Lu, and He 2013) with some changes. The imagery original pixel values were firstly converted into at satellite radiances. Fast Line-of-sight Atmospheric Analysis of Hypercubes atmosphere correction was conducted to remove the signal from atmosphere.

The third step was separating the water into different SSC grades according to water reflectance value at NIR band, that is, high reflectance is corresponding to high SSC. The qualitative classification of Landsat water reflectance was conducted on each single image. The water reflectance of an image was divided into seven to eight grades, between the lowest and the highest reflectance value, with an equal space. The top three grades represent relatively high SSC and the final three grades represent low SSC. The areas that had a relatively high SSC in every image were defined as HSAs, while, relatively low SSC areas as LSAs. Every image has its own relative HSAs and LSAs which are just used to compare within each single image, not between images.

In order to reveal the SSC distribution which was influenced by tidal currents, we separated the 37 images into two groups, that is, flood group (including images captured during mid to late period of flood tide and the tide turning phase) and ebb group (including images captured during ebb and the beginning of flood), and averaged, respectively. The averaging was performed on every group separately, following the steps below: The images of each group were averaged into one image, in which, pixel value was the result of averaging pixels at the same position of the group. The averaged reflectance value was then divided into seven to eight different grades and so we obtained the HSAs (the top three grades) and LSAs (final three grades). During averaging, the pixel values of cloud covered area were replaced by the averaged value of all other images, in the same group, without cloud in the corresponding area.

2.3. The current data

To show the currents' main characteristics in Hangzhou Bay, the tidal currents were simulated using the Regional Ocean Modelling System model (ROMS, Rutgers version 3.2, http://www.myroms.org/) (Song and Haidvogel 1994). Details of the ROMS computational algorithms are suggested by Shchepetkin and McWilliams (2005). The model results have been well validated by comparing the observations from S1 in Figure 1(*b*) in this study.

3. Results

3.1. SSC distribution and tidal currents in Hangzhou Bay

The qualitative SSC retrieved from Landsat data shows four HSAs in study area (Figures 2(*a*)(*1*)–(*c*)(*1*) and 3(*a*)–(*b*)). The HASs change with the tidal currents obviously (Figure 2(*a*)(*2*)–(*c*)(*2*)).

In Hangzhou Bay, the currents are dominated by semidiurnal tide, so usually the tide in any day can show the currents' main characteristics. Here we take three typical stages of the tidal currents on 1 July 2010 as examples, that is, in early flood, mid to late period of flood tide and ebb phase (Figures 2(*a*)(*3*)–(*c*)(*3*)).

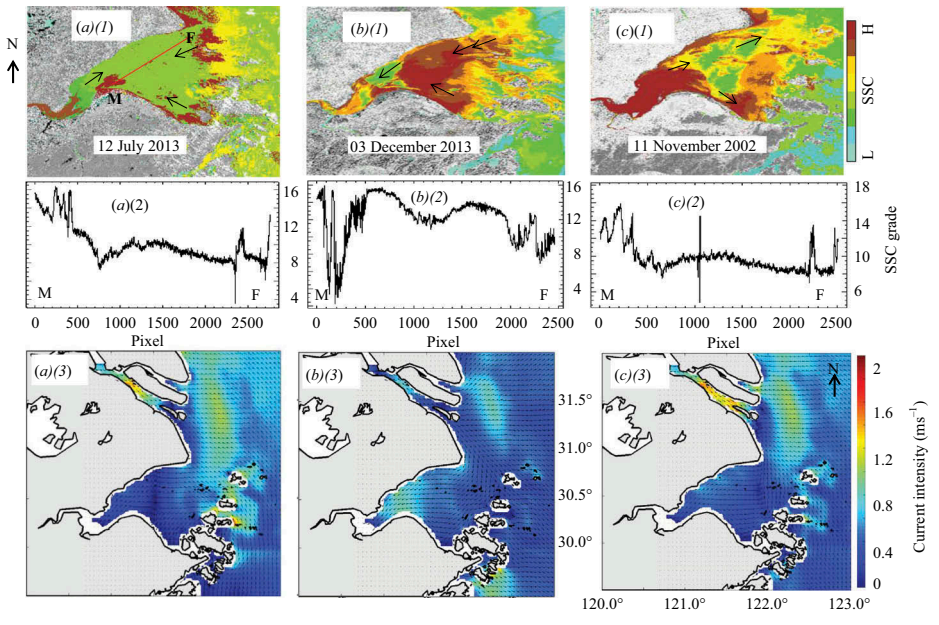

Figure 2. Qualitative SSC retrieved from Landsat data and simulated tidal currents during different stages. (*a*)(*1*)–(*a*)(*3*) Early flood block, that is, during the first 3 hours of flood. (*b*)(*1*)–(*b*)(*3*) Mid to late flood, that is, during mid to late period of flood tide; (*c*)(*1*)–(*c*)(*3*) Ebb block, that is, during ebb period. (*a*)(*1*)–(*c*)(*1*) Qualitative SSC retrieved from Landsat images. Black arrow: direction of local current. (*a*)(*2*)–*c*)(*2*) SSC changing trends along transects of MF; Horizontal axis: pixel number from point M. L: Low SSC; H: High SSC. (*a*)(*3*)–(*c*)(*3*) Tide currents in Hangzhou Bay on 1 July 2010 (Black arrow: the current direction). Colour bar: magnitude of flow intensity (ms^{-1}).

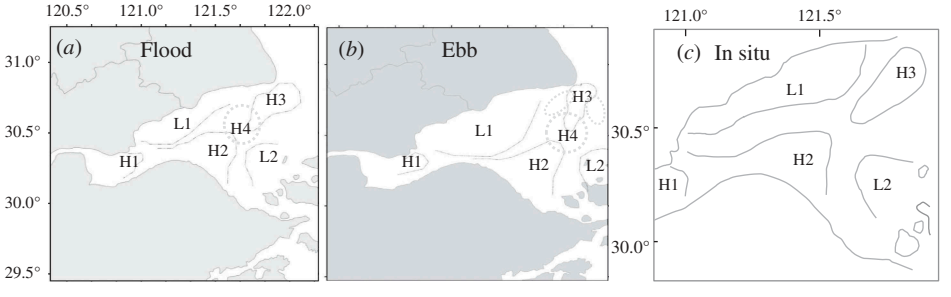

Figure 3. (*a*)–(*b*) Averaged SSC distribution map retrieved from satellite data during flooding (*a*) and ebbing (*b*). (*c*) Averaged SSC distribution obtained by averaging the observed SSC during spring tides in winter and summer (ECCHE, 1992; Xie et al. 2013). (H1–H4): High SSC areas numbered 1–4. (L1–L2): Low SSC areas numbered 1–2.

The tidal current continuously changes its direction and speed (Figure 2). During flood tide, especially during the mid to late period of flood tide, the water flow westward (Figures 2(*b*)(*3*)), the HSAs distribute at the west end of Hangzhou Bay, the south part of the bay, the northeastern part and near the middle of the bay (Figure 2 (*b*)(*1*) and 3(*a*)). During ebbing, except for the first HSA (west one), all the HSAs move eastward (Figure 3(*b*)).

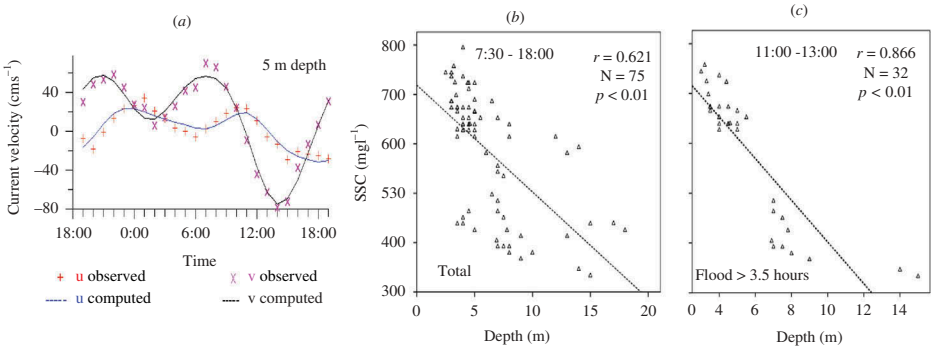

Figure 4. (*a*) The tidal current comparisons between model results and diurnal current observations (5 m depth) at one site on 4 and 5 August 2010, marked as S1 in Figure 1(*b*). Horizontal axis: Time. Vertical axis: u and v are x and y components of 5 m depth averaged velocity (ms^{-1}). (*b*)–(*c*) The correlation between in-situ SSC and water depth sampled on 30 March 2014, during the period from the beginning of flood to the end of ebb (7:30–18:00) (*b*), and during mid to late period of flood (11:00–13:00) (*c*). Flood > 3.5 hours: during mid to late period of flood. r: The correlation coefficient. p: Significance. y-axis: In-situ measured SSC (mgl^{-1}). The x-axis: Water depth, that is, ADCP measured value subtracted the tide height induced by tide.

Our comparison between model results and diurnal current observations at 5 m depth showed that model simulated currents are in good agreement with the observations (Figure 4(*a*)).

3.2. *The correlation of in-situ SSC and water depth*

The bathymetry of Hangzhou Bay in Figure 1(*b*) shows three main shallow areas (purple colour in Figure 1(*b*)) with the depth of approximately 2–7 m.

The SSC distribution map shows that HSAs are corresponding well with shallow water areas, while LSAs are corresponding well with deep water areas (Figures 3(*a*), (*c*) and 1(*b*)). The correspondence is better during the mid to late period of flood tide.

Further analysis showed a negative correlation (Figure 4(*b*)) between in-situ SSC and the water depth (ADCP measured value subtracted tide height induced by tide). The negative correlation is especially obvious during the mid to late period of flood tide (Figure 4(*c*)).

4. Discussions

4.1. *Tidal currents influence on SSC distribution*

Suspended sediments are mainly transported by the currents. Prior research from in-situ observation found that SSC increases with the increase of the currents speed (Xie et al. 2013). Under normal circumstances, the maximum tidal currents' speed in Hangzhou Bay during flooding is higher than that during ebbing and the maximum SSC often follows the maximum peak of tidal currents' speed with a lag of 1–1.5 hours (Chen and Wang 2008; Xie et al. 2013). Our results are in agreement with previous studies.

During flooding the tidal currents flow westward converging into the bay. Tide currents and flows with high suspended sediment from Yangtze River and the sediments re-suspension play an important role in forming the HSAs (Figures 2(*b*)(*1*), 3(*a*) and 3(*c*)).

When ebbing, the re-suspension process is comparatively weak and the water flow outward (dispersing) of the bay leading most of the middle area of the Bay to be hollow (low SSC) (Figures 2(*c*)(*1*) and 3(*b*)).

4.2. Other factors impact on SSC distribution

Seasonal winds can also affect SSC distribution in the Hangzhou Bay. In prior research, higher SSC water-leaving radiance was observed in the winter than that in the summer in Hangzhou Bay (Wang, Tang, and Shi 2007), and this is partly because seasonal monsoon winds and the ocean surface layer mixing effects (Shenliang, Guoan, and Shilun 2003).

Comparing to tidal current and river runoff, the influence of wind on SSC distribution in Hangzhou Bay is weaker (Li, Mao, and Zhang 2009). Even with the superposition of the influence of seasonal change on the entire Hangzhou Bay, the relative HASs and LSAs induced by topography together with phase of tidal current and river runoff still exist in each image. We can see the significant relationship between topography and SSC distribution from Landsat images in different phase of tidal current.

Based on the analysis above, general information on the seabed topography in Hangzhou Bay can be observed from SSC spatial distribution retrieved from satellite data, and it is better during mid to late term of flooding tide. Relatively high SSC area denotes low water depth area, while, most relatively low SSC areas are corresponding to deep water regions.

5. Conclusions

Analysis of Landsat OLI\TM\ETM+ data found four HSAs and two LSAs in Hangzhou Bay. During the mid to late period of flood tide, the HSAs are corresponding well with uplift areas of ocean floor with shallow water, while LSAs are distributed in deep water areas. SSC is negatively correlated with water depth. This can help us estimate the topography information. During ebbing, except for the first HSA (west one), all the HSAs move eastward.

Topography and the tidal currents together with river injection can significantly influence the spatial-temporal distribution of SSC. Besides the above factors, seasonal winds can also contribute to SSC distribution in Hangzhou Bay to some extent.

Acknowledgements

The Center for Earth Observation and Digital Earth, Chinese Academy of Sciences provided Landsat TM and OLI data. The views, opinions, and findings contained in this report are those of the authors and should not be construed as an official NOAA or U.S. Government position, policy or decision.

Disclosure statement

No potential conflict of interest was reported by the authors.

Funding

This work was supported by the Key Program of National Natural Sciences Foundation of China under Grant 41430968; China Petroleum & Chemical Corporation under Grant 313099; and Research project Natural Science Foundation of Zhejiang province under Grant LQ14D060001.

References

Chen, B., and K. Wang. 2008. "Suspended Sediment Transport in the Offshore near Yangtze Estuary." *Journal of Hydrodynamics, Ser. B*. 20 (3): 373–381. doi:10.1016/S1001-6058(08)60070-0.

ECCHE (Editorial Committee for Chinese Harbors and Embayments). 1992. *Chinese Harbors and Embayments (Part V)* [In Chinese]. Beijing: China Ocean Press.

Ilyina, T., T. Pohlmann, G. Lammel, and J. Sündermann. 2006. "A Fate and Transport Ocean Model for Persistent Organic Pollutants and Its Application to the North Sea." *Journal of Marine Systems* 63 (1–2): 1–19. doi:10.1007/BF02837889.

Jiang, X., B. Lu, and Y. He. 2013. "Response of the Turbidity Maximum Zone to Fluctuations in Sediment Discharge from River to Estuary in the Changjiang Estuary (China)." *Estuarine, Coastal and Shelf Science* 131: 24–30. doi:10.1016/j.ecss.2013.07.003.

Jilan, S., and W. Kangshan. 1989. "Changjiang River Plume and Suspended Sediment Transport in Hangzhou Bay." *Continental Shelf Research* 9 (1): 93–111. doi:10.1016/0278-4343(89)90085-X.

Li, N., Z. Mao, and Q. Zhang. 2009. "The Impact of Physical Processes on Pollutant Transport in Hangzhou Bay." *Chinese Journal of Oceanology and Limnology* 27: 266–276. doi:10.1007/s00343-009-9118-y.

Mayer, L. M., R. G. Keil, S. A. Macko, S. B. Joye, K. C. Ruttenberg, and R. C. Aller. 1998. "Importance of Suspended Participates in Riverine Delivery of Bioavailable Nitrogen to Coastal Zones." *Global Biogeochemical Cycles* 12 (4): 573–579. doi:10.1029/98GB02267.

Qiu, Z. F. 2013. "A Simple Optical Model to Estimate Suspended Particulate Matter in Yellow River Estuary." *Optics Express* 21 (23): 27891–27904. doi:10.1364/oe.21.027891.

Shchepetkin, A. F., and J. C. McWilliams. 2005. "The Regional Oceanic Modeling System (ROMS): A Split-Explicit, Free-Surface, Topography-Following-Coordinate Oceanic Model." *Ocean Modelling* 9 (4): 347–404. doi:10.1016/j.ocemod.2004.08.002.

Shenliang, C., Z. Guoan, and Y. Shilun. 2003. "Temporal and Spatial Changes of Suspended Sediment Concentration and Resuspension in the Yangtze River Estuary." *Journal of Geographical Sciences* 13 (4): 498–506. doi:10.1007/BF02837889.

Song, Y., and D. Haidvogel. 1994. "A Semi-Implicit Ocean Circulation Model Using A Generalized Topography-Following Coordinate System." *Journal of Computational Physics* 115 (1): 228–244. doi:10.1006/jcph.1994.1189.

Tang, D. L., I. Ni, F. Müller-Karger, and Z. Liu. 1998. "Analysis of Annual and Spatial Patterns of CZCS-Derived Pigment Concentration on the Continental Shelf of China." *Continental Shelf Research* 18 (12): 1493–1515. doi:10.1016/S0278-4343(98)00039-9.

Wang, F., B. Zhou, X. Liu, G. Zhou, and K. Zhao. 2012. "Remote-Sensing Inversion Model of Surface Water Suspended Sediment Concentration Based on In Situ Measured Spectrum in Hangzhou Bay, China." *Environmental Earth Sciences* 67 (6): 1669–1677. doi:10.1007/s12665-012-1608-0.

Wang, M., J. Tang, and W. Shi. 2007. "Modis-Derived Ocean Color Products along the China East Coastal Region." *Geophysical Research Letters* 34: L06611. doi:10.1029/2006GL028599.

Webster, T., and C. Lemckert. 2002. "Sediment Resuspension within a Microtidal Estuary/Embayment and the Implication to Channel Management." *Journal of Coastal Research* 36: 753–759.

Xie, D.-F., S. Gao, Z.-B. Wang, and C.-H. Pan. 2013. "Numerical Modeling of Tidal Currents, Sediment Transport and Morphological Evolution in Hangzhou Bay, China." *International Journal of Sediment Research* 28 (3): 316–328. doi:10.1016/S1001-6279(13)60042-6.